

Eggshell Assembly in *Drosophila*: Processing and Localization of Vitelline Membrane



[Metadata, citation and similar papers](#)

Provided by Elsevier - Publisher Connector

T. Pascucci,* J. Perrino,† A. P. Mahowald,† and G. L. Waring*¹

**Department of Biology, Marquette University, WLS 109, P. O. Box 1881, Milwaukee, Wisconsin 53201-1881; and †Department of Molecular Genetics/Cell Biology, University of Chicago, Chicago, Illinois 60637-1432*

The *Drosophila* eggshell consists of three major proteinaceous layers: the vitelline membrane, the inner chorionic layer, and the outer endochorion. During the latter stages of oogenesis, the proteins that comprise these layers are synthesized and secreted by epithelial follicle cells which surround the maturing oocyte. While there is considerable knowledge of the structural units which comprise the eggshell layers, there is little knowledge of how individual proteins function or interact with one another to form the structure. Immunoelectron microscopy was used to follow the distribution of four different eggshell proteins in the assembling and mature eggshell. sV23 and sV17, follicle cell proteins synthesized during the early stages of eggshell formation (stages 8–10), were distributed within the vitelline membrane layer at all stages. Despite marked temporal differences in their accumulation profiles, s36 and s18, putative chorion proteins, were similarly distributed throughout the floor, pillars, and roof of the endochorion. Although the vitelline membrane appears to be morphologically complete by stage 11, developmental Western blots and immunolocalization data indicate that molecular dynamism persists within the layer throughout the subsequent choriogenic stages. During early chorion formation the vitelline membrane appears to act as a reservoir for chorion proteins since s36 was found predominantly in the vitelline membrane layer of stage 12 egg chambers. During the late choriogenic stages (13–14), both sV17 and sV23 are processed to smaller derivatives. Interactions between the eggshell layers were suggested by ultrastructural analysis of a sV23 protein null mutant which showed that the structural integrity of the outer chorion is dependent upon the presence of a vitelline membrane component. © 1996 Academic Press, Inc.

INTRODUCTION

We are studying eggshell formation in *Drosophila* in order to elucidate how elaborate extracellular structures in higher eukaryotes are assembled from their secreted components. Recent studies implicating the vitelline membrane layer of the *Drosophila* eggshell as a repository of developmental information important for embryonic axis determination (St. Johnston and Nusslein-Volhard, 1992; Hong and Hashimoto, 1995) provide additional impetus for studying the nature and dynamics of protein–protein interactions within the eggshell layers.

The *Drosophila* eggshell is a multilayered, multiregional structure produced by ovarian follicle cells during the latter

stages of oogenesis (Margaritis, 1985). Relative to the oocyte surface, these layers include the proximal vitelline membrane, an inner chorionic layer (ICL), and a tripartate endochorion consisting of a thin floor, pillars, and a roof network. Autoradiographic studies suggest that the eggshell is assembled by apposition of newly synthesized proteins upon existing layers (Giorgi, 1977). Accordingly, eggshell proteins synthesized during the early stages of eggshell formation (stages 8–10) are considered putative vitelline membrane proteins, while those synthesized during the terminal stages of oogenesis (stages 11–14) are considered putative chorion components. Analyses of eggshell mutants suggest a more complex assembly pathway. Several female sterile mutations affecting eggshell assembly have been described; however, only three have been mapped to eggshell structural gene loci: *cor-36*, *fs(2)QJ42*, and *dec-1*. *cor-36* maps to a small region on the X chromosome (Digan *et al.*, 1979) which contains a cluster of eggshell structural genes that

¹ To whom correspondence should be addressed. Fax: (414) 288-7357. E-mail: waringg@vms.csd.mu.edu.

are expressed during the early stages of chorion formation (Parks and Spradling, 1987). Females homozygous for *cor 36* fail to synthesize s36, a putative chorion protein, and, as expected, produce eggshells with structural abnormalities in the endochorion layer (Digan *et al.*, 1979). *fs(2)QJ42* maps to region 26A of the second chromosome (Savant and Waring, 1989), a region which includes a small cluster of putative vitelline membrane protein genes (Popodi *et al.*, 1988). Females homozygous for *fs(2)QJ42* fail to accumulate sV23, a putative vitelline membrane protein, and produce eggshells with altered permeability properties (Savant and Waring, 1989), a phenotype associated with vitelline membrane defects. Like sV23, *dec-1* proteins are synthesized during the stages of vitelline membrane formation; however, females which fail to synthesize detectable quantities of the *dec-1* proteins display morphological abnormalities in the chorion layers (Bauer and Waring, 1987; Komitopoulou *et al.*, 1988). The endochorion layer fails to organize and collapses into the vitelline membrane layer during late choriogenesis. These *dec-1* mutants suggest that there is no strict correlation between a protein's time of synthesis, its localization, and its role in eggshell assembly.

In an effort to add molecular definition to the eggshell, we have adopted an immunological approach. Using polyclonal antibodies directed against four different eggshell proteins, we have localized two vitelline membrane proteins and two chorion proteins in the assembling and mature eggshell. We have also shown that vitelline membrane proteins are processed in a stage-specific manner and that the morphological integrity of the outer chorion layers is dependent upon proper expression of at least one vitelline membrane component, sV23.

MATERIALS AND METHODS

Production of trp E Fusion Proteins

Selected regions from cloned eggshell genes were subcloned in frame into pATH expression vectors (Koerner *et al.*, 1991). For sV23, a 330-bp *PstI* fragment encoding amino acids 26–136 (Popodi *et al.*, 1988) was first subcloned in a 5' to 3' orientation into a *PstI*-cut pGem 3 vector. Making use of appropriately placed *HindIII* and *SalI* sites in the polylinker region, the sV23 insert was excised and subcloned into a modified pATH-2 vector, pATH-2a (Nogueron and Waring, 1995). For sV17, a 250-bp *XmnI*–*PvuII* fragment encoding amino acids 3 to 84 (Burke *et al.*, 1987) was subcloned in a 5' to 3' orientation into the *SmaI* site of pGEM-3. Making use of appropriately positioned *EcoRI* and *HindIII* sites in the polylinker region, the sV17 fragment was cloned into pATH-2a. For s36 and s18, gel-purified restriction fragments from lambda genomic clones (Spradling *et al.*, 1981) were used as templates for polymerase chain reactions. A 675-bp fragment encoding the C-terminal 211 amino acids of s36 was amplified from a 4.0-kb *EcoRI* fragment using 5'-GGAATTCGAGGAGGCCCGTCGTTTGGGTCG-3' as the 5' primer and 5'-GCTCTAGAACAACCCATGCCAGGATGAGC-3' as the 3' primer. Ten million copies of template were denatured at 95°C for 3 min and then amplified for 30 cycles at 94°C for 30 sec, 58°C for 30 sec, and 70°C for 1 min. The extension time was

lengthened to 5 min on the last cycle. *Taq* polymerase (Promega) was used for all PCRs. After the ends of the PCR product were filled with Klenow fragment, the engineered *EcoRI* site at the 5' end of the PCR fragment was cut with *EcoRI*. The digested fragment was subcloned into an *EcoRI*- and *SmaI*-cut pGEM-3 vector. Making use of an appropriately placed *SalI* site in the polylinker region, the s36 sequences were excised as an *EcoRI/SalI* fragment and cloned into pATH-2a. For s18, a 272-bp fragment encoding the C-terminal half of s18 (amino acids 93–172) was amplified from a 2.2-kb *XbaI* gel-purified genomic fragment. Using 5'-CGAATTCGGCGGTGCCACCAGTCGATGCC-3' as a primer, a synthetic *EcoRI* site was introduced into the 5' end of the PCR product. The 3' end of the fragment was primed with 5'-GCTCTAGAC-AACGTTTTGCCACTTACTAGC-3'. The ends of the s18 PCR product were filled, and the s18 fragment was subcloned into pATH-2a as described previously for s36. All PCR constructs were verified by DNA sequence analysis.

Production of Antisera

trpE fusion proteins were induced in DH5 α transformants as previously described (Nogueron and Waring, 1995). Bacterial lysates prepared according to Sambrook *et al.* (1989) were fractionated by preparative SDS-PAGE. *trpE* fusion proteins were excised and electroeluted as previously described (Nogueron and Waring, 1995), emulsified in an equal volume of Freund's complete adjuvant, and injected at multiple subcutaneous sites into New Zealand white rabbits. One month after the primary injection (200 μ g fusion protein), the rabbits were boosted at monthly intervals with 100–150 μ g of fusion protein emulsified in Freund's incomplete adjuvant. The sera were collected and processed by standard procedures (Harlow and Lane, 1988). The sV23 antiserum was purified by adsorption to acetone powders prepared from *fs(2)QJ42* mutant ovaries. *fs(2)QJ42* females fail to accumulate the sV23 eggshell protein (Savant and Waring, 1989). Ovaries used for the acetone powders were resuspended in 0.9% NaCl at 1 g (wet weight) per milliliter, disrupted by sonication, and mixed with four volumes of cold acetone (–20°C). The precipitated protein was collected by centrifugation (12,000g, 15 min), washed, air dried, and incubated with antiserum diluted in PBS. Acetone powders were incubated for 2 to 5 hr at room temperature with the diluted antiserum. For immunolocalizations, an acetone powder from 200–300 ovary equivalents was used for each microliter of undiluted serum that was adsorbed.

Western Blot Analysis of Egg Chamber Extracts

Ovaries were dissected in insect Ringer's (130 mM NaCl, 4.7 mM KCl, 1.9 mM CaCl₂, 10 mM Hepes, pH 7.0) at room temperature. Egg chambers were pooled according to stage and solubilized in Laemmli sample buffer (Laemmli, 1970). Following the removal of insoluble material by centrifugation, the soluble egg chamber proteins were resolved on 16% polyacrylamide gels by SDS-PAGE. Proteins were electrophoretically transferred (E. C. Apparatus Corp.) to nitrocellulose or PVDF membranes at 4°C in buffer containing 25 mM Tris, 190 mM glycine, and 20% methanol. After transfer at 0.2 A for 16–20 hr the blots were air dried. The nitrocellulose blots were processed as described in Harlow and Lane (1988); the PVDF membranes were processed according to the manufacturer's instructions (NEN-Dupont). Blots were incubated at room temperature overnight with diluted antisera, washed, and incubated with ¹²⁵I-rProtein A (New England Nuclear) in blocking buffer (0.05

$\mu\text{Ci } ^{125}\text{I}$ -rProteinA/lane). Radiolabeled blots were washed, air dried, and exposed to X-ray film at -70°C .

Immunolocalizations

Ovaries from wild-type (Oregon R, P2 strain) or mutant females were removed in cold insect Ringer's and fixed in 0.06 M sodium phosphate buffer, pH 7.2–7.4, containing 2% formaldehyde and 1% glutaraldehyde. Following fixation overnight at 4°C , the ovaries were rinsed in 60 mM sodium phosphate, pH 7.2, containing 0.2 M sucrose. Rinsed ovaries were dehydrated in a graded series of ethanol solutions at progressively lower temperatures: 30% at 4°C ; 50% at 0°C ; 70%, 95%, and 100% at -20°C (1 hr for each solution). The final dehydration step in 100% ethanol was done at -20°C for a minimum of 12 hr. Tissue was infiltrated with Lowicryl K4M resin in a graded Lowicryl:ethanol series (1:1; 2:1, and 1:0). Each step was at -20°C for 1.5 hr. A final infiltration step in 100% resin was done at 4°C for 3 days. Following infiltration, the samples were polymerized in fresh resin under UV light in a UVC2 cryo chamber (Ted Pelco) operated at -20 to -25°C . After 3 days at -20°C , UV polymerization was continued at room temperature for an additional 3 days. Thin sections mounted on nickel grids coated with formvar and carbon were blocked overnight in PBS containing 2% BSA. Blocked grids were incubated at room temperature with primary antibody diluted in blocking buffer for 1.5 to 2 hr. After a brief wash with PBS, the grids were incubated with secondary antibody [20 nm gold coupled to goat anti-rabbit IgG (Polysciences, Inc.)] for 1.5 hr. Following postfixation (1% glutaraldehyde, 1% formaldehyde in PBS) for 30 min, grids were washed and stained with uranyl acetate (15 sec) and lead citrate (15 sec) prior to their examination with a JEOL 100CX II transmission electron microscope.

RESULTS

Accumulation of Eggshell Antigens

mRNAs encoding the putative vitelline membrane proteins sV17 and sV23 are synthesized during stages 8–11 and 8–10 of oogenesis, respectively (Popodi *et al.*, 1988) with peak accumulation of both newly synthesized proteins in stage 10 egg chambers (Fagnoli and Waring, 1982). Maximal synthesis of the early chorion protein, s36, occurs during stages 12 and 13, while synthesis of the late chorion protein, s18, is predominant in stage 14 egg chambers (Waring and Mahowald, 1979). Western blots of staged egg chamber extracts incubated with each of the four antisera (sV17, sV23, s36, and s18) show reactive bands with the expected stage specificities (Fig. 1). The s18 antiserum recognizes a single species in the size range 18 kDa, which accumulates in stage 13 and 14 egg chambers. A single prominent band in the size range 36 kDa is observed in stages 11–14 with the s36 antisera. While the antisera to the putative chorion proteins recognized proteins of the expected size, the putative vitelline membrane antisera recognized species in the expected size ranges only during the early stages of eggshell formation (9–10a); during the later stages of oogenesis the reactive species were smaller than expected. In early stage 10 egg chambers, the sV23 antisera gave a relatively sharp

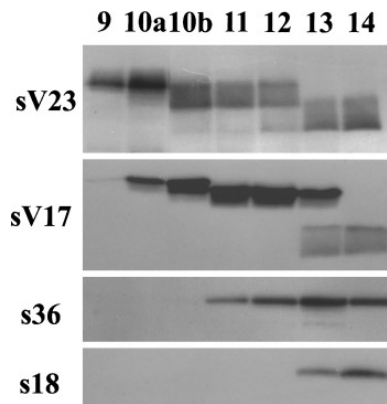


FIG. 1. Accumulation of eggshell antigens during the terminal stages of oogenesis. Extracts from staged egg chambers (9–14) were resolved on four independent SDS polyacrylamide gels (16%) and transferred to nitrocellulose (sV23, sV17) or PVDF membranes (s36, s18). Each blot was reacted with diluted antisera (1:1000) directed against the eggshell fusion protein indicated at the left. 50 and 20 egg chambers per lane were used for the vitelline membrane protein antisera, sV23 and sV17, respectively; 10 egg chambers per lane were used for the s36 and s18 antisera. The sizes of the reactive species were estimated based on their migration relative to proteins of known molecular sizes run in parallel: bovine serum albumin, 68 kDa; ovalbumin, 43 kDa; carbonic anhydrase, 29 kDa; and lysozyme, 14.3 kDa.

signal in the size range 23 kDa. As the development of the stage 10 egg chambers progressed, the 23-kDa signal became smeared. A change in the mobility of the smear was clearly detected in late stage 10 egg chambers (10b). The leading edge of the smear migrated in the size range 21 kDa, while the trailing edge remained in the size range 23 kDa. The mobilities of the reactive species remained unchanged until stage 13. In stage 13 and 14 egg chambers, the mobility of the reactive smear increased with the leading edge migrating in the size range 17 kDa. A similar profile of changes in the mobilities of the reactive species was seen with the sV17 antisera. Aside from changes in the mobilities of the reactive species, decreases in the intensities of the reactive species were seen in late stage egg chambers, particularly with the sV17 antisera. The decreased intensities could reflect loss of epitopes or changes in their solubilities. During late oogenesis eggshell proteins become covalently cross-linked and are no longer soluble in SDS buffers (Spradling, 1993).

Stage-Specific Processing of Vitelline Membrane Antigens

The stage-specific appearance of faster migrating species with the sV23 and sV17 antisera is consistent with either developmentally regulated processing or early insolubilization of the vitelline membrane antigens, coupled with cross reactivity of the antisera to smaller chorion proteins synthe-

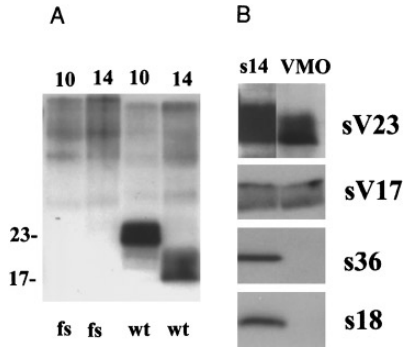


FIG. 2. The sV23 and sV17 antisera recognize processed vitelline membrane antigens. (A) SDS soluble proteins from wild-type (wt) and female sterile *fs(2)QJ42* (*fs*) mutant egg chambers (stages 10 and 14) were resolved by SDS-PAGE. Proteins were transferred to a nitrocellulose membrane and reacted with sV23 antisera (1:1000 dilution). The *fs* samples contained 103 egg chambers/lane; wt samples contained 40 egg chambers/lane. The approximate sizes (kDa) of the reactive species are indicated at the left. (B) Independent Western blots of extracts from whole (s14) and dechorionated stage 14 egg chambers (VMO) were reacted with antisera raised against the eggshell fusion proteins indicated at the right. Chorions were mechanically removed by rolling the stage 14 egg chambers over double-stick tape. The effectiveness of the method was verified by the failure to detect signals in the s18 and s36 VMO lanes.

sized during the late stages of oogenesis (e.g., s15, s16, s18, s19). To verify the specificity of the sV23 antisera, we made use of a previously characterized female sterile mutant, *fs(2)QJ42*, which fails to synthesize detectable amounts of the sV23 vitelline membrane protein (Savant and Waring, 1989). As shown in Fig. 2A, reactive species in the size ranges 23 and 17 kDa are not detected with the sV23 antisera in either stage 10 or 14 mutant egg chambers. The failure to detect a faster migrating species in the stage 14 egg chambers suggests that sV23 is processed to a smaller derivative during late oogenesis. Although direct evidence for sV17 processing is not available, the retention of the stage 14 sV17 signal in vitelline membrane/oocyte preparations is consistent with processing of a vitelline membrane antigen (Fig. 2B). Unlike the small sV23 and sV17 reactive antigens, the s36 and s18 chorion proteins are no longer detected when chorions are mechanically removed from stage 14 egg chambers.

Stage-specific processing of eggshell proteins is not unprecedented. The *dec-1* eggshell gene encodes three isoforms, each of which is cleaved in a developmentally regulated manner during the terminal stages of oogenesis (Nogueron and Waring, 1995). Conservation of the complex *dec-1* processing pathways in distantly related species (Nogueron, unpublished results) suggests that proteolytic processing is functionally significant. Figure 3 shows that processing of the vitelline membrane antigens is also conserved in evolution. As in *Drosophila melanogaster*, the sV17 antisera recognizes antigens in the size range 17 kDa in *D.*

yakuba (20 Myr diverged) and *D. virilis* (60 Myr diverged) stage 10 egg chambers and smaller 14-kDa forms in stage 14 egg chambers. All three species also showed similar profiles with the sV23 antisera. The additional band in the size range 13–14 kDa, which was detected in the *D. virilis* lanes, was also observed in overexposed blots of *D. melanogaster* egg chambers. This band does not appear to be a derivative of sV23 since it is also present in overexposed blots of *fs(2)QJ42* mutant egg chambers (data not shown).

Loss of sV23 Epitopes during Late Oogenesis

To determine the distribution of sV23 and its derivative, sectioned egg chambers were reacted with the sV23 serum and processed for immunogold analysis. Gold particles were localized over the vitelline membrane in stage 10 and stage 14 egg chambers (Figs. 4A and 4C) while labeling of the chorion layer was at background levels (Fig. 4B). Although our Western blot analyses indicated that sV23 and its 17-kDa derivative were the predominant reactive species (Fig. 2A), to verify the specificity of the sV23 serum *in situ* the serum was reacted with sectioned *fs(2)QJ42* egg chambers. As shown in Fig. 4D there was substantial labeling of the vitelline membrane in this sV23 protein null mutant. Taken together with Figs. 4B and 4C, this indicates that the sV23 serum contains antibodies that recognize epitopes which are also present on other vitelline membrane components. To remove the cross-reacting antibodies, the sV23 serum was preadsorbed with an acetone powder prepared from *fs(2)QJ42* ovaries. When incubated with the preadsorbed serum, immunogold particles over the *fs(2)QJ42* vitelline membrane were reduced to background levels (stage 13, Fig.

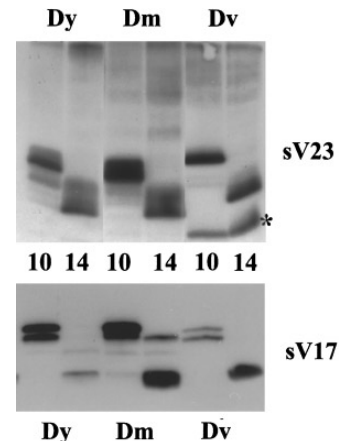


FIG. 3. Processing of sV23 and sV17 is conserved in evolution. Western blots of SDS soluble proteins from stage 10 and stage 14 egg chambers were incubated with the sV23 (top) and sV17 antisera (bottom). The two lanes to the left are from *D. yakuba* (Dy); the middle lanes are from *D. melanogaster* (Dm); and the far right lanes are from *D. virilis* (Dv). An additional cross-reacting band at approximately 14 kDa in the Dv lanes is marked by an asterisk.

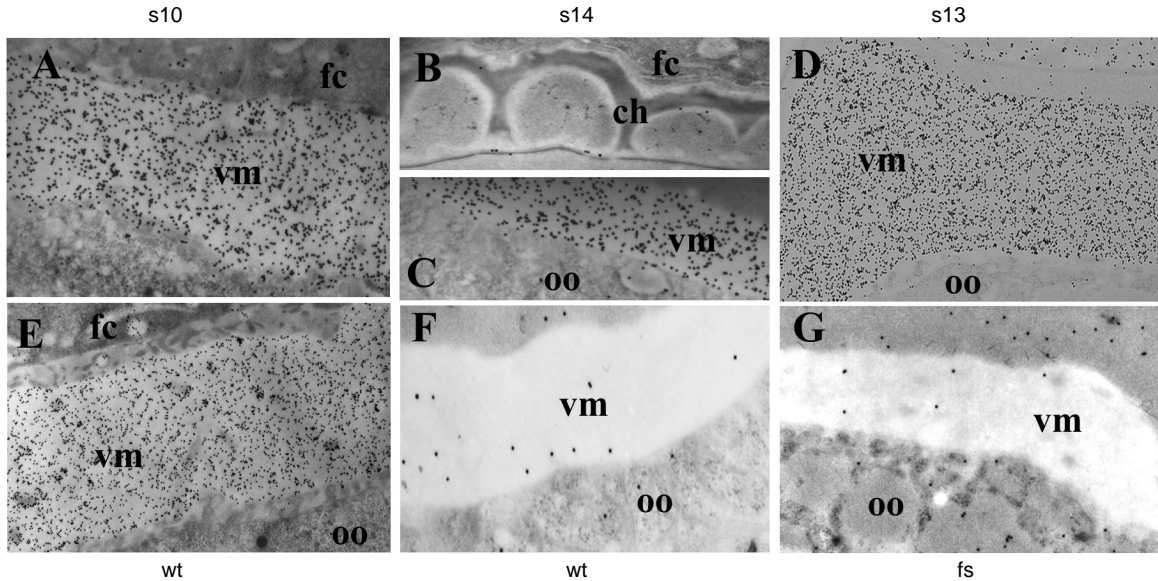


FIG. 4. Immunogold staining of the vitelline membrane with sV23 antiserum. 90- to 95-nm sections showing the vitelline membrane and chorion of wild-type (wt) and *fs(2)QJ42* (fs) egg chambers reacted with sV23 (A–D) and sV23 preadsorbed serum (E–G) at the following dilutions: (A,B,C,E,F) 1:8000; (D,G), 1:800. The egg chamber stages are shown at the tops of the columns. vm, vitelline membrane; fc, follicle cell; oo, oocyte; ch, chorion. (Magnifications: A, $\times 5000$; B, $\times 8500$; C, $\times 12000$; D, $\times 9500$; E, $\times 5000$; F, $\times 17500$; G, $\times 13000$.)

4G; stage 10, not shown). The preadsorbed serum selectively stained the vitelline membrane in wild-type stage 10 egg chambers as expected (Fig. 4E), but failed to stain the stage 14 egg chambers (Fig. 4F). This result suggests a loss or change in the accessibility of sV23 epitopes in late stage egg chambers.

To test for a loss of sV23 epitopes in late stage egg chambers, parallel lanes from a Western blot containing extracts of mixed stage 10 and 14 egg chambers were incubated with preadsorbed sV23 serum (Fig. 5). As shown in lanes 3 and 4 there is a significant reduction in the intensity of the stage 10 signal and a loss of the stage 14 signal when the sV23 serum was preadsorbed with acetone powder from 10 *fs(2)QJ42* ovary equivalents (lane 4). The intensity of the stage 10 signal was maintained when the serum was preadsorbed with *fs(2)QJ42* powder from 50 or 100 ovary equivalents (lanes 5 and 6, respectively). These data indicate that the larger stage 10 protein contains epitopes which are not present in the cross-reacting material and that antibodies in the sV23 serum which recognize epitopes in the region that is retained in the smaller stage 14 form cross-react with proteins in the *fs(2)QJ42* acetone powder. Taken together our results suggest that after preadsorption, the remaining sV23-specific antibodies recognize epitopes which are present on the larger 23-kDa form, but which are removed when sV23 is processed to its smaller 17-kDa derivative. This suggests that the lack of immunogold labeling with the preadsorbed sV23 serum seen in Fig. 4F reflects loss, rather than masking, of vitelline membrane epitopes in stage 14 egg chambers.

Localization of Eggshell Antigens in the Assembling and Mature Eggshell

The distribution of the sV17, s36, and s18 antigens in the assembling and mature eggshell is shown in Fig. 6. For sV17, gold particles are selectively concentrated in the vitelline membrane in stage 10 and 12 egg chambers. While gold particles remain concentrated in the vitelline membrane through stage 14, the density of gold particles is dramatically reduced in late stage egg chambers (panel 2 vs 4). s36

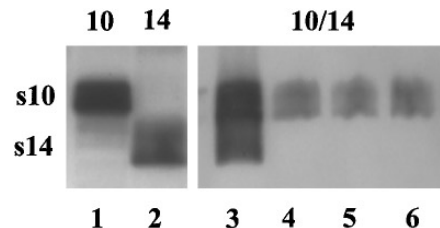


FIG. 5. Loss of sV23 epitopes in stage 14 egg chambers. Lanes 1 and 2 show a Western blot of SDS soluble proteins from stage 10 and 14 egg chambers incubated with sV23 antiserum. The positions of the stage 10 (s10) and stage 14 (s14) sV23 signals are indicated to the left. Lanes 3–6 are from a Western blot of mixed egg chamber stages (13 stage 10 and 13 stage 14/lane) reacted with sV23 (lane 3) or sV23 preadsorbed serum (lanes 4–6). Acetone powders from *fs(2)QJ42* ovaries equivalent to 10, 50, and 100 ovarian equivalents were used to absorb the sV23 serum in lanes 4 through 6, respectively.

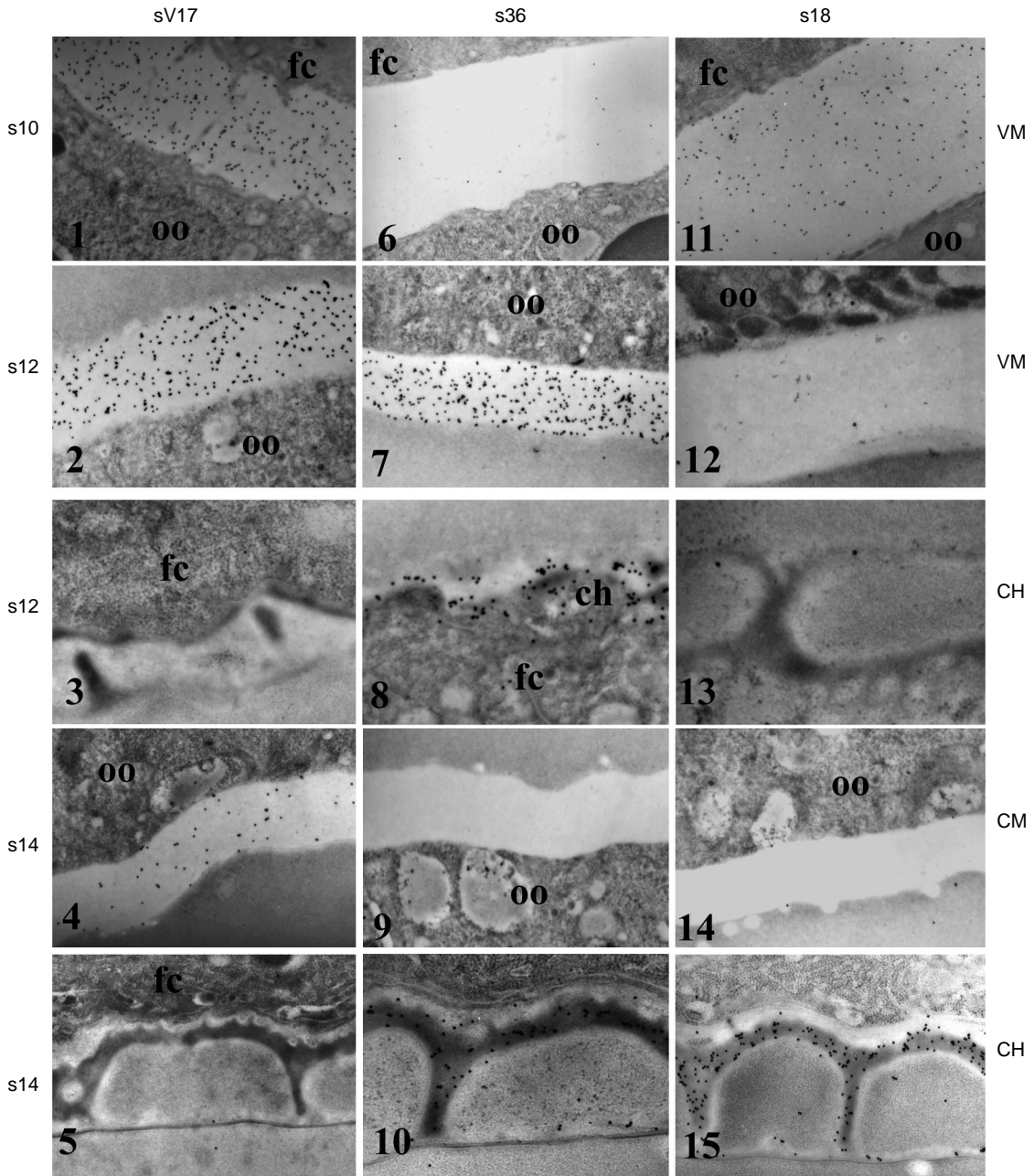


FIG. 6. Immunogold labeling of the vitelline membrane and chorion eggshell layers with the sV17, s36, and s18 antisera. Thin-sectioned egg chambers at the stages shown on the left were reacted with the sV17 (column I), s36 (column II), or s18 (column III) antisera. All sections were incubated with 1:8000 dilutions of the antisera except section 15 which was incubated with a 1:500 dilution. The eggshell layer shown in each row is indicated at the right. Staging was based upon morphological criteria which included the relative size of the oocyte to the entire egg chamber, the length of the chorionic appendages, and the fine structure of the follicle cells and the developing endochorion. Since eggshell production by the follicle cells is not synchronous there are spatial asymmetries in the extent to which the endochorion layers have developed within a single egg chamber. The differences in the appearance of the endochorion in the stage 12 preparations reflects this spatial asymmetry. For the sV17 and s18 antisera, sections were taken from a region near the anterior pole of a late stage 12 egg chamber; the less developed s36 section was taken from the same egg chamber near the posterior pole. The anterior-to-posterior progression of eggshell development has been previously documented (Margaritis, 1986). The sV17 stage 10 section was taken from an early stage 10 egg chamber, while the s36 and s18 sections were taken from late stage 10 egg chambers. (oo, oocyte; fc, follicle cell; ch, chorion) (Magnifications: 1, 2, $\times 16,000$; 3, $\times 24,000$; 4, $\times 14,000$; 5, $\times 17,000$; 6, $\times 7,200$; 7-9, $\times 20,000$; 10, $\times 18,500$; 11, $\times 11,000$; 12, $\times 25,000$; 13, $\times 28,000$; 14, $\times 17,000$; 15, $\times 20,000$.)

is not detected in stage 10 egg chambers (panel 6). During the early stages of endochorion deposition (stage 12), s36 gold particles are concentrated in follicle cell secretory vesicles, the developing chorion, and the vitelline membrane (panels 7, 8). In early stage 14 egg chambers, gold particles are localized in the pillars, floor, and roof of the endochorion complex (panel 10) and are no longer detected in the vitelline membrane (panel 9). The transient appearance of s36 in the vitelline membrane suggests that a significant fraction of the early s36 secretions fails to become incorporated into the assembling endochorion or that the vitelline membrane serves as an extracellular reservoir for early s36 secretions from which s36 is released at a later time for assembly into the developing endochorion. If the vitelline membrane-associated secretions do not participate in endochorion assembly, the proteins must be degraded since the vitelline membrane is cleared of s36 by late stage 13. Substantial turnover of s36 during terminal oogenesis is not compatible with the accumulation profile shown in Fig. 1. Although s18 does not begin to accumulate until stage 13 (Fig. 1), gold particles are detected with the s18 serum in the vitelline membrane of stage 10 egg chambers (panel 11). Since no cross-reacting material was detected on our Western blots, the cross-reactivity observed *in situ* may reflect a cross-reacting structural epitope. As seen in panels 12 and 14, gold particles are not detected in the vitelline membranes of more mature egg chambers, suggesting that structural changes occur within the vitelline membrane layer after its apparent morphological completion at stage 11 (Margaritis, 1985). Panel 13 shows that the pillar, roof, and floor substructure of the developing endochorion are apparent in the anterior regions of late stage 12/early stage 13 egg chambers. s18 was not detected in this roof structure, suggesting that a roof framework is established by the early chorion proteins prior to the secretion of s18. In late stage 13 and early stage 14 egg chambers, when s18 becomes detectable in follicle cell secretory granules, gold particles are localized in the endochorion roof and pillar apices (data not shown). In middle to late stage 14 egg chambers, s18 is distributed throughout the endochorion complex (panel 15). In previous morphological studies the substructures of the floor, roof, and pillars were indistinguishable (Margaritis, 1986), which suggested similar biochemical compositions. The colocalization of s18 and s36 is consistent with these observations and suggests that late chorion proteins are intercalated into a previously formed endochorion framework. Despite a distribution similar to s36, s18 by itself does not appear to be capable of organizing a proper endochorion framework. Female sterile mutants (*cor 36*) which fail to produce detectable quantities of s36 form totally disorganized endochorion structures (Digan et al., 1979).

sV23 Vitelline Membrane Protein Is Required for the Stabilization of the Outer Chorion Layers

To investigate potential intermolecular or interlayer interactions, we studied the distribution of sV17, s36, and s18

in the sV23 protein null mutant, *fs(2)QJ42* (Fig. 7). As in wild type, sV17 appears to be evenly distributed throughout the vitelline membrane layer in stage 10 egg chambers. In stage 14 egg chambers, sV17-associated gold particles remain within the vitelline membrane; however, the continuity of the layer is disrupted by clumps of electron-dense material. While the tripartate structure of the endochorion typical of wild type is observed at earlier stages (data not shown), by middle to late stage 14 the dense accumulations in the vitelline membrane are accompanied by a severely disrupted endochorion complex. As shown in Fig. 7, s36 and s18 accumulate both in the electron-dense particles within the vitelline membrane and in the remnants of the endochorion complex.

DISCUSSION

A relationship between eggshell proteins synthesized during the period of vitelline membrane formation and stabilization of the endochorion complex during late oogenesis has been previously documented in studies of *dec-1* female sterile mutants (Bauer and Waring, 1987). The *dec-1* eggshell gene encodes three primary translation products which are synthesized by the follicle cells predominantly during stages 9–11 of oogenesis (Waring et al., 1990). In *dec-1* mutants, an organized endochorion complex fails to form and endochorion material collapses into the vitelline membrane during stage 14. Formation and collapse of the endochorion complex appear to be separable events. In *cor 36* mutant egg chambers, an organized endochorion complex fails to form, yet endochorion material is not found in the vitelline membrane (Digan et al., 1979). On the other hand, in the sV23 null mutant *fs(2)QJ42*, an organized endochorion complex is formed initially but collapses into the vitelline membrane during late stage 14. Since sV23 epitopes were detected only within the vitelline membrane (Fig. 4B, C), stabilization of the outer chorion layers appears to be dependent at least in part on a properly formed vitelline membrane layer. How a vitelline membrane protein such as sV23 influences protein–protein interactions in the outer chorion layers remains unknown. The timing of the collapse in mutant egg chambers is similar to the timing of the loss of sV23-specific epitopes in wild-type egg chambers (Figs. 4 and 5). Late stage processing of sV23 may precipitate structural changes within the vitelline membrane layer which are transmitted to the chorionic layers via as-yet unknown mechanisms. If the sV23-specific epitopes which are no longer detected in stage 14 egg chambers are released as a peptide, this peptide could provide a molecular link between the vitelline membrane and the assembling chorion layers. Since we did not observe sV23 epitopes in the endochorion complex (Fig. 4B), a transient association must be postulated.

The distribution of the 17-kDa sV23 derivative within the vitelline membrane layer could not be definitively established with our sV23 serum. The sV23 serum contains

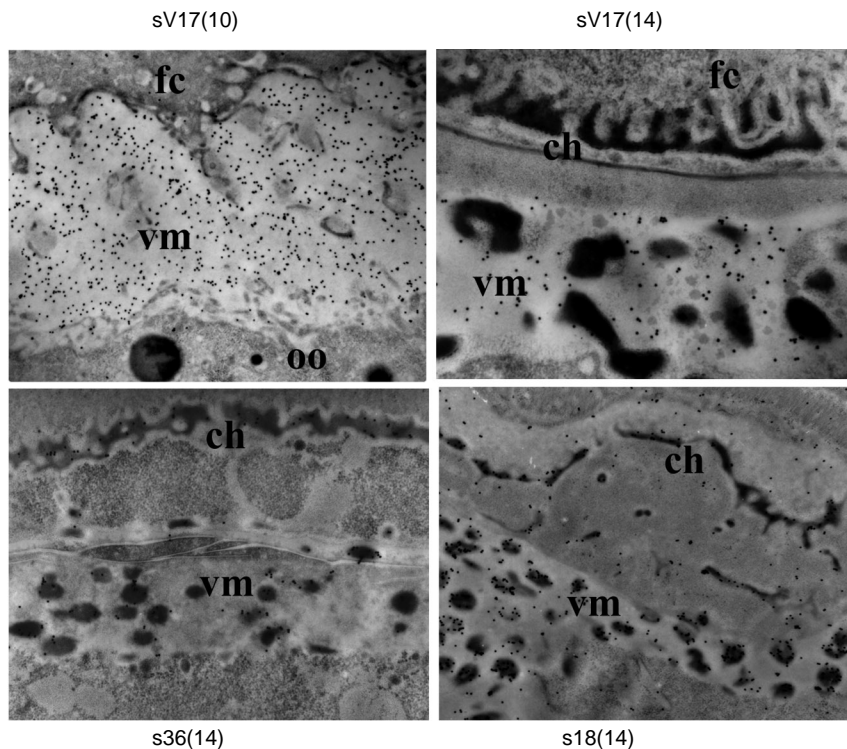


FIG. 7. Endochorion proteins collapse into the vitelline membrane in a *sV23* vitelline membrane protein mutant. Immunogold analysis of thin sections through the eggshell layers of stage 10 and stage 14 *fs(2)QJ42* mutant egg chambers reacted with sV17, s36, or s18 antisera. The stage 14 sections show anterior regions of the main shell. All antisera were diluted at 1:8000 except s18 which was diluted at 1:500. Within the vitelline membrane, s18 and s36 gold particles were selectively localized over the electron-dense globules. (vm, vitelline membrane; fc, follicle cell; oo, oocyte; ch, chorion.) Magnifications: sV17(10), $\times 10,500$; sV17(14), $\times 21,000$; s36(14), $\times 16,500$; s18(14), $\times 12,000$.

antibodies which recognize *sV23*-specific epitopes as well as *sV23* epitopes which are present on other vitelline membrane components (Fig. 4). Since the *sV23*-specific epitopes recognized by our antiserum are removed when *sV23* is processed to its 17-kDa derivative, localization of this derivative will require a serum which recognizes *sV23*-specific epitopes in the 17-kDa protein. The fusion protein used to generate our *sV23* serum included amino acids 27 to 136 of the pre-pro-protein. The C-terminal residues (137–168) may contain *sV23*-specific epitopes which are not removed when *sV23* is processed to its 17-kDa derivative.

Like *sV23*, *sV17* was processed in a stage-specific manner. Although we have not yet documented the loss of *sV17* epitopes in late stage egg chambers, the faster mobility and reduced intensity of the *sV17* Western blot signals in stage 14 egg chambers (Fig. 1) and the decreased density of *sV17*-associated gold particles in stage 14 vitelline membranes (Fig. 6) are all consistent with a late cleavage event. Many secreted proteins are synthesized as pre-pro-proteins. In several cases site-specific proteolysis of pro-proteins occurs at sites marked by basic amino acids (Lindberg and Hutton, 1991). Inspection of the conceptual translations of *sV17* and *sV23* revealed potential monobasic sites (RLRK and RVSR in *sV17* and *sV23*,

respectively) in the N-terminal regions of both proteins which were found within a sequence context characteristic of documented monobasic cleavage sites (Devi, 1991). The *sV23* and *sV17* sites are also potential targets for furin, a Kex 2 protease homolog (Hatsuzawa *et al.*, 1992; Molloy *et al.*, 1992). Interestingly, a *Drosophila* furin homolog, dKLIP-1, is expressed in both the follicle cells and oocyte (Hayflick, 1992). Once the *sV17* and *sV23* processing sites are identified, we can begin to address the functional significance of these post-translational modifications with the *sV23* protein. Since *sV23* null mutants are available, it should be possible to remove defined target sites by site-directed mutagenesis and test the functional significance of these alterations in the *fs(2)QJ42* mutant background by P-element-mediated transformation experiments. In this way, a functional link between vitelline membrane processing and chorion morphogenesis can be tested.

REFERENCES

- Bauer, B. J., and Waring, G. L. (1987). 7C female-sterile mutants fail to accumulate early eggshell proteins necessary for later chorion morphogenesis in *Drosophila*. *Dev. Biol.* 121, 349–358.

- Burke, T., Waring, G. L., Popodi, E., and Minoo, P. (1987). Characterization and sequence of follicle cell genes selectively expressed during vitelline membrane formation in *Drosophila*. *Dev. Biol.* 124, 441–450.
- Devi, L. (1991). Peptide processing at monobasic sites. In "Peptide Biosynthesis and Processing" (L. D. Fricker, Ed.). CRC Press, Boca Raton, FL.
- Digan, M. E., Spradling, A. C., Waring, G. L., and Mahowald, A. P. (1979). The genetic analysis of chorion morphogenesis in *Drosophila melanogaster*. In "Eucaryotic Gene Regulation ICN-UCLA Symposium" (R. Axel et al., Eds.), pp. 171–181. Academic Press, New York.
- Fagnoli, J., and Waring, G. L. (1982). Identification of vitelline membrane proteins in *Drosophila melanogaster*. *Dev. Biol.* 92, 306–334.
- Giorgi, F. (1977). An EM autoradiographic study on ovarian follicle cells of *Drosophila melanogaster* with special reference to the formation of egg coverings. *Histochemistry* 52, 105–117.
- Harlow, E., and Lane, D. (1988). "Antibodies: A Laboratory Manual." Cold Spring Harbor Laboratory Press, Cold Spring Harbor, NY.
- Hatsuzawa, K., Nagahama, M., Takahashi, S., Takada, K., Murakami, K., and Nakayama, K. (1992). Purification and characterization of furin, a kex2-like processing endoprotease, produced in Chinese hamster ovary cells. *J. Biol. Chem.* 267, 16094–16099.
- Hayflick, J. S., Wolfgang, W. J., Forte, M. A., and Thomas, G. (1992). A unique kex 2-like endoprotease from *Drosophila melanogaster* is expressed in the central nervous system during early embryogenesis. *J. Neurosci.* 12, 705–717.
- Hong, C. C., and Hashimoto, C. (1995). An unusual mosaic protein with a protease domain, encoded by the nudel gene, is involved in defining embryonic dorsoventral polarity in *Drosophila*. *Cell* 82, 785–794.
- Koerner, T. J., Hill, J. E., Myers, A. M., and Tzagoloff, A. (1991). High-expression vectors with multiple cloning sites for construction of trpE-fusion genes: pATH vectors. *Methods Enzymol.* 194, 477–490.
- Komitopoulou, K., Gans, M., Margaritis, L., and Kafatos, F. C. (1983). Isolation and characterization of sex-linked female-sterile mutants in *Drosophila melanogaster* with special attention to egg-shell mutants. *Genetics* 105, 897–920.
- Komitopoulou, K., Margaritis, L. H., and Kafatos, F. C. (1988). Structural and biochemical studies on four sex-linked chorion mutants of *Drosophila melanogaster*. *Dev. Genet.* 9, 37–48.
- Laemmli, U. K. (1970). Cleavage of structural proteins during the assembly of the head of bacteriophage T4. *Nature (London)* 227, 680–685.
- Lindberg, I., and Hutton, J. C. (1991). Peptide processing proteinases with selectivity for paired basic residues. In "Peptide Biosynthesis and Processing" (L. D. Fricker, Ed.). CRC Press, Boca Raton, FL.
- Margaritis, L. (1986). The eggshell of *Drosophila melanogaster*. II. New staging characteristics and fine structural analysis of choriogenesis. *Can. J. Zool.* 64, 2152–2175.
- Margaritis, L. H. (1985). Structure and physiology of the eggshell. In "Comprehensive Insect Physiology, Biochemistry and Pharmacology" (G. A. Kerkurt and L. I. Gilbert, Eds.), Vol. 1, pp. 153–173. Pergamon, New York.
- Molloy, S. S. et al. (1992). Human furin is a calcium-dependent serine endoprotease that recognizes the sequence arg-X-X-arg and efficiently cleaves Anthrax protective antigen. *J. Biol. Chem.* 267, 16396–16402.
- Noguerón, M. I., and Waring, G. L. (1995). Regulated processing of *dec-1* eggshell proteins in *Drosophila*. *Dev. Biol.* 172, 272–279.
- Parks, S., and Spradling, A. (1987). Spatially regulated expression of chorion genes during *Drosophila* oogenesis. *Genes Dev.* 1, 497–509.
- Popodi, E., Minoo, P., Burke, T., and Waring, G. L. (1988). Organization and expression of a second chromosome follicle cell gene cluster in *Drosophila*. *Dev. Biol.* 127, 248–256.
- Sambrook, J., Fritsch, E. F., and Maniatis, T. (1989). "Molecular Cloning: A Laboratory Manual," Vol. 3, pp. 18.40–18.41. Cold Spring Harbor Laboratory Press, Cold Spring Harbor, NY.
- Savant, S. S., and Waring, G. L. (1989). Molecular analysis and rescue of a vitelline membrane mutant in *Drosophila melanogaster*. *Dev. Biol.* 135, 43–52.
- Spradling, A. C. (1981). The organization and amplification of two chromosomal domains containing *Drosophila* chorion genes. *Cell* 27, 193–201.
- Spradling, A. C. (1993). Developmental genetics of oogenesis. In "The development of *Drosophila melanogaster*" (M. Bates and A. Martinez Arias, Eds.), Vol. 1, pp. 1–70. Cold Spring Harbor Laboratory Press, Cold Spring Harbor, NY.
- St. Johnson, D., and Nüsslein-Volhard, C. (1992). The origin of pattern and polarity in the *Drosophila* embryo. *Cell* 68, 201–219.
- Waring, G. L., and Mahowald, A. P. (1979). Identification and time of synthesis of chorion proteins in *Drosophila melanogaster*. *Cell* 16, 589–598.
- Waring, G. L., Hawley, R. J., and Schoenfeld, T. (1990). Multiple proteins are produced from the *dec-1* eggshell gene in *Drosophila* by alternative RNA splicing and proteolytic cleavage events. *Dev. Biol.* 142, 1–12.

Received for publication January 17, 1996

Accepted May 7, 1996